# Novel application of 3D contrast-enhanced CMR to define fibrotic structure of the human sinoatrial node *in vivo*

**Author names:** Thomas A. Csepe[1], Jichao Zhao[2], Lidiya V. Sul[1], Yufeng Wang[2], Brian J. Hansen[1], Ning Li[1], Anthony J. Ignozzi[1], Anna Bratasz[1,3], Kimerly A. Powell[1,3], Ahmet Kilic[3,4], Peter J. Mohler[1,3,5], Paul M.L. Janssen[1,3,5], John Hummel[3,5], Orlando P. Simonetti[3,6], Vadim V. Fedorov[1,3]

**Affiliations:** 1- Department of Physiology & Cell Biology, The Ohio State University Wexner Medical Center, 304 Hamilton Hall, 1645 Neil Avenue, Columbus, OH 43210, USA; 2- Auckland Bioengineering Institute, The University of Auckland, 70 Symonds Street, Auckland 1142, New Zealand; 3- Davis Heart & Lung Research Institute, The Ohio State University Wexner Medical Center, 473 W 12th Avenue, Columbus, OH 43210, USA; 4- Department of Surgery, The Ohio State University Wexner Medical Center, 410 W. 10th Avenue, Columbus, OH 43210, USA; 5- Department of Internal Medicine, The Ohio State University Wexner Medical Center, 395 W 12th avenue, Columbus, OH 43210, USA; 6- Department of Biomedical Informatics, The Ohio State University Wexner Medical Center, 250 Lincoln Tower, 1800 Cannon Drive, Columbus, OH 43210, USA.

**Address for correspondence:** Vadim V. Fedorov, PhD
300 Hamilton Hall, 1645 Neil Avenue, Columbus OH 43210-1218
tel: 1-614-292-9892 fax: 1-614-292-4888 e-mails: vadim.fedorov@osumc.edu

## SUPPLEMENTAL METHODS

### *In vivo* LGE-CMR and fibrosis estimation

Volunteers underwent LGE-CMR scans using a 3T MAGNETOM Tim Trio (Siemens HealthCare) with a spatial resolution of 1.0mm$^3$ (Volunteers #1,3,4 and #5) or 0.625x0.625x1.25mm$^3$ (Volunteer #2). LGE-CMR scans were acquired 18-25min following 0.2 mmol/kg gadolinium agent injection. An ECG-gated, fat-suppressed 3D inversion recovery gradient recalled echo sequence with respiratory navigator gating was used. Typical scan parameters were as follows: echo time- 2ms, flip angle- 20$^0$, inversion time- 300ms, repetition time- 4.4ms, and receiver bandwidth- 355Hz/pixel, 8-10min scan time. 3D image data covering the entire heart including both atria and both ventricles were acquired and reformatted into 2D cross sections (1mm or 1.25mm thick, **Table S1**). Volunteer #1 was scanned a second time one year later to show the results from a scan with a different contrast agent and is referred to as Volunteer #1B (**Table 1** and **Figure 3**).

From *in vivo* LGE-CMR images, the atrial chamber walls were identified, segmented, smoothed to an isotropic resolution, and volume rendered as a 3D reconstruction using a custom-written Matlab (MathWorks Inc.) program and visualized in 3D using both Matlab and Amira programs (FEI Company) (**Figure 1**). Atrial wall thickness consisted of 2-5mm except interatrial septum (IAS), and crista terminalis (CT) region. Due to in-flow artifact in the pulmonary veins caused by navigator pulses for respiration gating, the left atrium (LA) was hyper-enhanced in some views, limiting analysis to only the RA (**Figure 1A**).

A patient-specific fibrotic mask was applied to the 3D LGE-CMR atrial structure (**Figure S1**). Signal intensity thresholds at standard deviations (SD) above the average RA free wall (RAFW) signal intensity, a low-intensity area that served as the signal intensity reference, were

considered areas of high intensity post contrast (**Figures 2-3**). These areas of high signal intensity were defined as fibrotic tissue in accordance with previously published atrial fibrosis quantification studies using a similar method(11;13). The heart-specific threshold for SAN LGE fibrosis was selected from within a range, as was done previously (14), to achieve a percent of fibrotic content within the SAN region consistent with reported values for healthy adult human hearts (35-55%)(6;9). **Table 1** shows fibrosis analysis for thresholds of 2, 2.5, 3, and 4 SD above the RAFW for each volunteer. Subsequently, fibrosis segments were used to distinguish the SAN from surrounding atrial regions by computing a finite difference grid mesh. Regional LGE percentage for the SAN, RAFW, and IAS was calculated by fractionating the area of LGE, based on the applied threshold, from total selected tissue area. 3D fibrosis density maps were constructed at each voxel by determining the percent of neighboring voxels above the threshold within a 5 pixel radius. The delineation of the medial SAN border was not always distinct due to the presence of fibrosis in SVC and IAS, which was consistent with *ex vivo* analysis. Thus, maximum SAN width was limited to 9 mm.

**Optical mapping of coronary-perfused human atrial preparations**

Patient-specific data can be found in **Table 2**. Explanted human hearts were cardioplegically-arrested and cooled to 4°C in the operating room following cross-clamping of the aorta. Hearts were stored in cold cardioplegic solution (4°C) during transport, dissection, and cannulation. Human atrial preparations were isolated as previously described (1;2), coronary-perfused and superfused with 36.5±0.5°C oxygenated Tyrode's solution under constantly maintained pH (7.35±0.05) and pressure (55±5mm Hg) (2;3). Thus, stable heart rhythm, atrial conduction, and repolarization were maintained in the entire preparation for 4-8 hours (1;2). The atrial preparations were immobilized with 10μM blebbistatin and stained with voltage sensitive, near-infrared dye di-4-ANBDQBS(2). All mapped atrial preparations excluded regions of poor coronary perfusion/ischemia.

In Heart #1, optical action potentials (OAPs) were recorded using a high-resolution (optical field-of-view 3.3x3.3cm$^2$, 330μm resolution) CMOS camera (MiCAM Ultima-L, SciMedia Ltd, CA; 100x100 pixels), both of which were focused on the epicardium. In Heart #2, the high-resolution CMOS camera and three panoramic CMOS cameras simultaneously recorded atrial signals from the epicardium. In the three lateral right atria preparations, Hearts #3-5, a dual-sided optical mapping system (endocardial and epicardial, 330μm$^2$ resolution, and panoramic, 940μm$^2$ resolution CMOS cameras (100x100 pixels), MiCAM Ultima-L, SciMedia Ltd, CA) developed by our laboratory was used to obtain simultaneous sub-endocardial and sub-epicardial intramural weighted OAPs. Excitation light simultaneously illuminated both surfaces to excite di-4-ANBDQBS such that each camera recorded intramural OAPs (1-4mm deep), specifically weighted from the sub-endocardial and sub-epicardial layers, to visualize intramural SAN signals (**Figure 4**). OAPs from the SAN and atria were analyzed using a custom Matlab computer program as previously described (4). Additionally, activation maps and movies were used to visualize SAN and atrial activation.

***Ex vivo* CE-CMR**

Following optical mapping, CE-CMR was performed on atrial preparations as previously described (5). CE-CMR and histology of *ex vivo* atria were used to define SAN within the lateral right atria (RA) structure as previously described (5). After the mapping experiments, RA were formalin fixed for 48-72 hours, then washed out with PBS and incubated at 4$^0$C in 0.2% Gd-DTPA (dimeglumine gadopentetate Magnevist, Bayer Schering Pharma) for 3-6 days in order to perform a post-contrast CE-CMR. Right atria were imaged using a 9.4T Bruker BioSpin Spectrometer (Ettlingen, Germany) and a 72mm volume coil. FLASH_3Dslab_bas protocol was used to obtain high-resolution images with the following parameters: echo time 2.4ms, repetition time 12.7ms, flip angle 45-55°, and number of averages = 4. Volume images with up to 90μm$^3$

resolution of regions 2.5x6x6cm$^3$ were obtained in 3-4 hours (**Figure 4D-E**). 2D CMR images of the SAN (**Figure 5**) were segmented and smoothed using a custom-written Matlab (MathWorks Inc.) program and visualized in 3D using both Matlab and Amira (FEI Company) (**Figure 4D-E**).

### ***Ex vivo*** **tissue dissection and staining**

In the *ex vivo* heart preparations (n=5), immunostaining and histological staining (n=5) were used to delineate SAN structural location. SAN activation maps were projected to the epicardial surface of preparations to guide SAN histological dissection (**Figure 5A)**. SAN pacemaker complex and surrounding atrial myocardium, including crista terminalis (CT), right atrial free wall (RAFW), superior vena cava (SVC) and interatrial septum (IAS), were formalin-fixed, paraffin-embedded and serial sectioned (5μm thick sections) from the epicardium to the endocardium as previously described(6). Roughly fifteen sections from each heart were stained with Masson's trichrome (Sigma Aldrich) for all *ex vivo* hearts. In Heart #1, Heart #3, and Heart #5, an average of five sections across the SAN head, center, and tail of each heart were immuno-labeled with Connexin43 (Cx43, Sigma Aldrich) and Vimentin (Abcam) or Cx43 and alpha-actinin (Abcam). Histology sections were imaged with a 20x digital slide scanner (0.5x0.5μm$^2$ resolution, Aperio ScanScope XT, Leica). High-resolution images of immuno-labeled slides were captured by an Olympus FV1000 Filter confocal (**Supplemental Figure S2A**), and whole slide images were imaged by a Typhoon 9410 imager (GE Healthcare) (**Supplemental Figure S2B**). Histology and immunostaining images were used to identify and delineate the SAN pacemaker tissue from the surrounding right atria based on positive (atrial myocardium) and negative (SAN) Cx43 expression, distinct cell morphology, cell diameter and percent tissue fibrosis as previously described by our group and other human *ex vivo* SAN studies(7-10).

## Reference List


(1) Fedorov VV, Glukhov AV, Ambrosi CM, Kostecki G, Chang R, Janks D, et al. Effects of KATP channel openers diazoxide and pinacidil in coronary-perfused atria and ventricles from failing and non-failing human hearts. *J Mol Cell Cardiol* 2011;51(2):215-25.

(2) Fedorov VV, Glukhov AV, Chang R, Kostecki G, Aferol H, Hucker WJ, et al. Optical mapping of the isolated coronary-perfused human sinus node. *J Am Coll Cardiol* 2010;56(17):1386-94.

(3) Fedorov VV, Chang R, Glukhov AV, Kostecki G, Janks D, Schuessler RB, et al. Complex interactions between the sinoatrial node and atrium during reentrant arrhythmias in the canine heart. *Circulation* 2010;122(8):782-9.

(4) Fedorov VV, Schuessler RB, Hemphill M, Ambrosi CM, Chang R, Voloshina AS, et al. Structural and functional evidence for discrete exit pathways that connect the canine sinoatrial node and atria. *Circ Res* 2009;104(7):915-23.

(5) Hansen BJ, Zhao J, Csepe TA, Moore BT, Li N, Jayne LA, et al. Atrial fibrillation driven by micro-anatomic intramural re-entry revealed by simultaneous sub-epicardial and sub-endocardial optical mapping in explanted human hearts. *Eur Heart J* 2015;36(35):2390-401.

(6) Csepe TA, Zhao J, Hansen BJ, Li N, Sul LV, Lim P, et al. Human sinoatrial node structure: 3D microanatomy of sinoatrial conduction pathways. *Prog Biophys Mol Biol* 2016;120(1-3):164-78.

(7) James TN. Anatomy of the human sinus node. *Anat Rec* 1961;141:109-39.

(8) Csepe TA, Kalyanasundaram A, Hansen BJ, Zhao J, Fedorov VV. Fibrosis: a structural modulator of sinoatrial node physiology and dysfunction. *Front Physiol* 2015;6:37.

(9) Chandler N, Aslanidi O, Buckley D, Inada S, Birchall S, Atkinson A, et al. Computer three-dimensional anatomical reconstruction of the human sinus node and a novel paranodal area. *Anat Rec (Hoboken)* 2011;294(6):970-9.

(10) Shiraishi I, Takamatsu T, Minamikawa T, Onouchi Z, Fujita S. Quantitative histological analysis of the human sinoatrial node during growth and aging. *Circulation* 1992;85(6):2176-84.

**Table S1 – *In vivo* Patient Data**

| Volunteer # | Sex | Age | Heart Status | LGE-CMR Resolution ($mm^3$) | Contrast Agent |
|---|---|---|---|---|---|
| 1A | M | 41 | Healthy | 1x1x1 | Magnevist |
| 1B | M | 42 | Healthy | 1x1x1 | Prohance |
| 2 | M | 23 | Healthy | 0.625x0.625x1.25 | Magnevist |
| 3 | M | 48 | Healthy | 1x1x1 | Prohance |
| 4 | M | 52 | Healthy | 1x1x1 | Prohance |
| 5 | M | 24 | Healthy | 1x1x1 | Prohance |

**Table S2 – *Ex vivo* Patient Data**

| Heart # | Heart ID | Sex | Age | Heart Weight (g) | Diagnosis (Cause of Death) | CE MRI Resolution ($\mu m^3$) |
|---|---|---|---|---|---|---|
| 1 | 749693 | F | 63 | 608 | None (MVA) | 110x125110 |
| 2 | 402879 | M | 65 | 643 | Hypertension (CVA/ICH) | 100x100100 |
| 3 | 364587 | M | 19 | 300 | None (MVA) | 90x90x90 |
| 4 | 415217 | M | 54 | 474 | Hypertension (ICB/ICH) | 100x100x100 |
| 5 | 947200 | M | 42 | 508 | None (ICB/ICH) | 178x184x359 |

Abbreviations: CVA- cerebrovascular accident; DM- diabetes mellitus; HTN-hypertension; ICB-intracerebral bleed; ICH-intracerebral hemorrhage; MVA- motor vehicle accident.

**Table S3- *In vivo* and *Ex vivo* SAN size**

| SAN Size | | | | | | | |
|---|---|---|---|---|---|---|---|
| ***In vivo*** | | | | ***Ex vivo*** | | | |
| **Volunteer #** | **Length** | **Width** | **Depth** | **Heart #** | **Length** | **Width** | **Depth** |
| 1A | 23.3 | 8 | 3.3 | 1 | 26.6 | 4.9 | 2.5 |
| 1B | 24.1 | 8.4 | 3 | 2 | 19 | 4.7 | 1.7 |
| 2 | 25.5 | 6.3 | 2.3 | 3 | 25.8 | 3.4 | 2 |
| 3 | 25 | 6.7 | 2.9 | 4 | 21.5 | 5.3 | 2.1 |
| 4 | 23.3 | 6.1 | 2.5 | 5 | 16.5 | 3.5 | 2.5 |
| 5 | 20.1 | 7.5 | 3.1 | | | | |
| | | | | | | | |
| Average | 23.6 | 7.2 | 2.9 | | 21.9 | 4.4 | 2.2 |
| SD | 1.9 | 0.9 | 0.4 | | 4.3 | 0.9 | 0.3 |

**Figure S1**

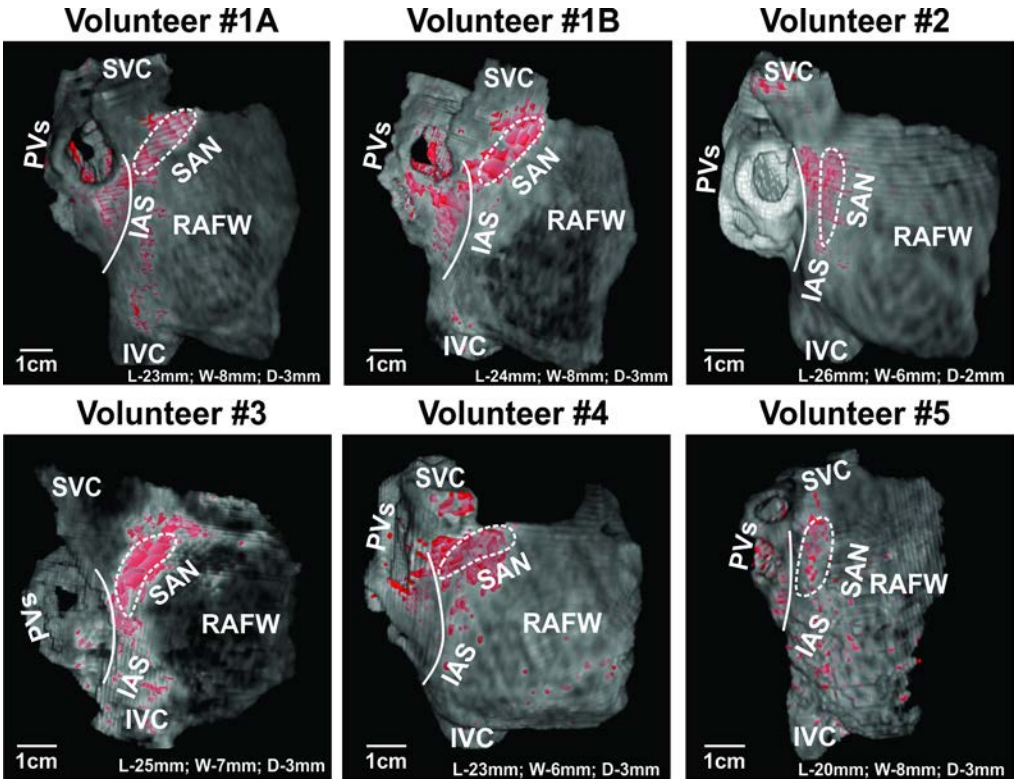


**Figure S1 *In vivo* SAN identification by LGE-CMR**

Lateral views of Volunteers #1-5 atrial reconstructions showing enhanced signal at the junction of the SVC and right atria corresponding to the anatomical location of the SAN. In Volunteer #1, enhanced regions are observed in similar locations in the first scan (#1A) and the second scan (#1B), which was performed over one year after the initial scan. Abbreviations; D- depth; IAS- interatrial septum; IVC- inferior vena cava; L- length; PVs- pulmonary veins; RAFW- right atrial free wall; SAN; sinoatrial node; SVC; superior vena cava; W-width.

**Figure S2**

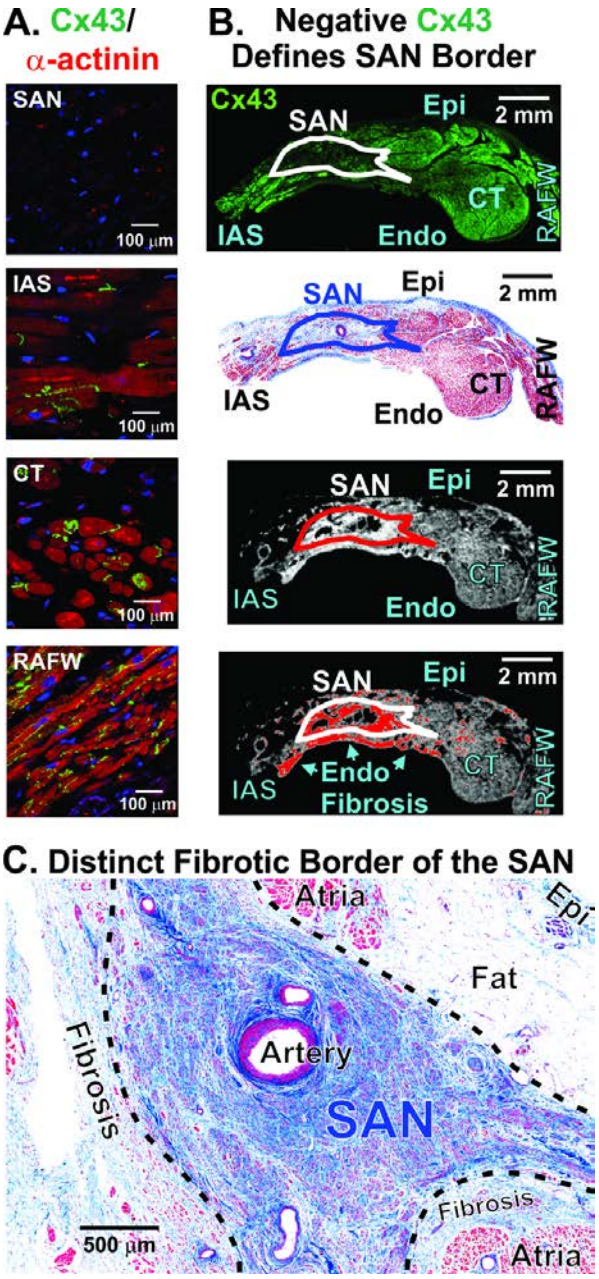


**Figure S2- Delineation of the Human SAN**

**A.** High resolution sections immunostained for connexin 43 (Cx43, green) and α-actinin (red) show Cx43 positivity in the interatrial septum (IAS), crista terminalis (CT), and right atrial free wall (RAFW). **B.** From top to bottom: Cx43 immunostained section with SAN outlined as Cx43

negative region; Masson's Trichrome stained section with SAN outlined as compact fibrotic region; 2D contrast-enhanced CMR (CE-CMR) image of the same section as histology with the histologically validated SAN border overlaid; 2D CE-CMR cross section with fibrosis enhancement mask applied shows fibrotic content within the SAN as well as adjacent endocardial layer. **C.** Masson's trichrome staining showing distinct SAN location based on dense fibrosis (blue) in SAN compared to surrounding atria, which is composed mainly of cardiomyocyte (red) tissue. Abbreviations as in Supplementary **Figure S1**; Endo- endocardium; Epi- epicadium.